HOLOS
ISSN 1807 - 1600

CHARACTERIZATION OF DIFFERENT SAMPLES OF THE GYPSUM MINERAL FROM THE ARARIPE GYPSUM POLE: FROM MACRO TO MICRO WITH RIETVELD REFINEMENT

E. C. SOUZA, R.A.P. OLIVEIRA, A.V. FERRAZ

Universidade Federal do Vale do São Francisco

edjancastro@hotmail.com

ORCID ID: https://orcid.org/0000-0002-1152-442X

Submitted March 14, 2023 - Accepted June 16, 2023

DOI: 10.15628/holos.2023.14902

ABSTRACT

The gypsum mineral is composed of calcium sulfate dihydrate and has as its main application the production of gypsum plaster. In the deposits of the Araripe gypsum pole there are, *in natura*, different varieties, identified by the names: "Johnson", alabaster, "estrelinha", "cocadinha", "rapadura" and "boró". The characterization of the varieties of gypsum in fracture was performed by SEM and the characterization of the powder was performed by FRX and DRX. By FRX, the presence of CaO was detected with a weight range of 42.5% to 47.1%, and SO_3 with a weight range of 48.1% to 53.2%. By XRD analysis, the majority gypsum phase was identified, with the presence of the crystalline planes characteristic of the mineral. From the refinement by the Rietveld method a $\chi 2$ result between 0.86 and 1.11 was obtained, and it was possible to obtain information about the microstructure of the gypsum varieties and their unit cell.

KEYWORDS: Gypsum Mineral, X-ray Diffraction, X-ray Fluorescence, Rietveld Method, Araripe Gypsum Pole.

CARACTERIZAÇÃO DE DIFERENTES AMOSTRAS DO MINERAL GIPSITA DO POLO GESSEIRO DO ARARIPE: DO MACRO AO MICRO COM REFINAMENTO RIETVELD

RESUMO

O mineral gipsita é composto por sulfato de cálcio di-hidratado e tem como principal aplicação a produção de gesso. Nas jazidas do polo gesseiro do Araripe ocorrem, *in natura*, diferentes variedades, identificadas pelos nomes: "Johnson", alabastro, "estrelinha", "cocadinha", "rapadura" e "boró". A caracterização das variedades de gipsita em fratura foi realizada por MEV e a caracterização do pó foi realizada por FRX e DRX. Por FRX, a presença de CaO foi detectada com uma variação de 42,5% a 47,1% em massa, e SO_3 com uma variação de 48,1% a 53,2% em massa. A partir da análise por DRX, foi identificada a fase maioritária de gipsita, com a presença dos planos cristalinos característicos do mineral. A partir do refinamento pelo método Rietveld obteve-se um resultado $\chi 2$ entre 0,86 e 1,11, e a partir deste, obter informações sobre a microestrutura das variedades de gipsita e sua célula unitária.

PALAVRAS-CHAVE: Mineral Gipsita, Difração de raios-X, Fluorescência de raios-X, Método Rietveld, Polo Gesseiro do Araripe.

1 Introduction

Gypsum is a calcium sulfate dihydrate ($CaSO_4.2H_2O$) in which the calcium (Ca) and sulfur (S) needed for its formation are derived from the rock erosion and transported by waters that precipitate the mineral. Precipitation by evaporation of groundwater becomes propitious in arid environments and shallow saline lakes. Gypsum is composed of the following chemical elements: calcium (Ca), sulfur (S), oxygen (O) and hydrogen (H), where the proportions in oxides and the crystallization water content are as follows: calcium oxide (CaO, 32.6 %), sulfur trioxide (SO_3, 46.5 %) and crystallization water (H_2O, 20.9%) by weight (Sharpe & Cork, 2006).

The gypsum *in natura* is formed by crystals of the monoclinic crystal system with face-centered cubic (FCC) unit cell and may also present different types of crystals, such as tubular, prismatic and lenticular forms (Silva & Giulietti, 2010).

According to Klein & Dutrow (2012) the most well-known mineralogical varieties of gypsum are: satin spar, which presents a sly glow and fibrous appearance; alabaster, which is finely granulated with fibrous aspect and widely used in sculptures; and, selenite, placose, colorless and translucent variety.

The industry's great interest in gypsum mineral is due to its characteristic in easily dehydrating. In the calcination process, gypsum loses its water of crystallization at an initial temperature of approximately 90 °C, and up to about 180 °C, it takes the form of calcium sulfate hemidrate ($CaSO_4.\ 1/2H_2O$) (Bouzit et al, 2019).

The phases that constitute the sulfate water system are: gypsum ($CaSO_4.2H_2O$), bassanite ($CaSO_4.1/2H_2O$) and anhydrites ($CaSO_4$) α, β and γ (Schmid et al., 2020).

According to Sharp and Cork (2006), in its calcined form, the gypsum has applications in the production of hemihydrates α and β. The hemihydrate β is a product that, when rehydrated, has high plasticity, until set, at which time it begins to obtain mechanical resistance. The α is obtained through autoclave calcination, under controlled pressure and temperature, with the use of higher purity gypsum varieties. Calcination under these conditions produces dense and ordered crystals.

The microstructure of materials can be observed by using the X-ray diffraction (XRD) technique with the help of mathematical models, such as the Rietveld method (MR), to decipher the crystal structure and unit cell details (Young, 1993; Rietveld, 1969).

The unit cell of gypsum has a monoclinic crystalline system structure, formed by layers interconnected by hydrogen bonds. The water of crystallization present in the composition of the mineral is evidenced by the hydrogen bond, formed by the hydrogen of the water molecule and the oxygen of the sulfate groups (Henry et al., 2009).

In the Araripe Gypsum Pole, the gypsum varieties presented, known as (a) “Johnson”, a variety characterized by presenting a structure with nodules and stars can be found; (b) alabaster of fibrous aspect, with white color; (c) “estrelinha” with star-shaped radiating crystals; (d)

HOLOS
ISSN 1807 - 1600

“cocadinha”, stratified gypsum with rare green clay films; (e) “rapadura”, variety of darker coloration, stratified into thicker layers; (f) "boró", also known as floor ore, a material that occurs forming a mixture of alabaster and clay, found in the cover of deposits (Oliveira et al., 2012).

Lins (2018) reports that the Araripe gypsum Pole provides raw material for 95% of the Brazilian gypsum production, due to the ease of extraction and logistics.

Taking into account these data that report the relevance of the mineral to the region, added to the fact that there are no studies that characterize, microstructurally, these different types of gypsums, this work aims to characterize by scanning electron microscopy, X-ray fluorescence and X-ray diffraction, with refinement by Rietveld method, different samples of rock gypsums from Araripe gypsum Pole to verify the purity and microstructural characteristics.

2 Methodology

A field visit was made to the Araripe gypsum Pole in the city of Ouricuri located in the state of Pernambuco (Brazil) to collect samples of the different types of gypsum mineral, having as object of study the following varieties, as illustrated in Figure 1.

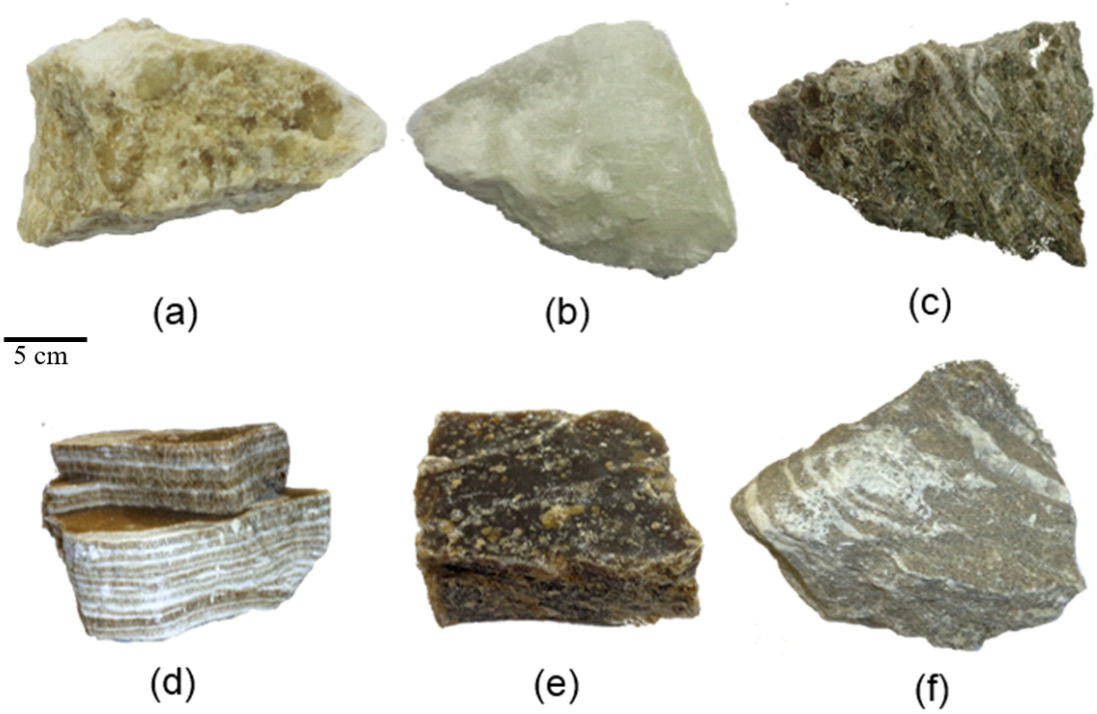

Figure 1: Mineralogical varieties of rock gypsum: (a) Johnson, (b) alabaster, (c) estrelinha, (d) cocadinha, (e) rapadura and (f) boró.

The samples were ground individually in a TECNAL ball mill model TE-350, with a speed of 617 revolutions/minute, for 1.5 min until powder was obtained. The ground samples were sieved

by separating the granulometry between 150 µm and 75 µm (100 and 200 mesh, respectively) for characterization by X-ray fluorescence and X-ray diffraction.

In order to analyze the morphology, the fractured samples were metallized with gold (Au) using the Quorum equipment model Q150R ES with a current of 15mA/5min. Micrographs were obtained with a TESCAN electron microscope, model VEGA 3XMU.

The semi-quantitative determination of the chemical composition of the samples was obtained by XRF of the powdered samples using the EdX-720 Shimadzu equipment operating at 50 kV and 30 mA under vacuum, with a rhodium (Rh) metal tube.

X-ray diffraction (XRD) measurements were taken a powder diffractometer Xpert Pro MPD - Panalytical, with Co-Kα radiation (λ=1.7889 Å), with the tube operating at 40 kV/40 mA and reading from 5° to 90° in 2θ.

The X'Pert HighScore Plus (2006) software was used to identify crystalline phase and convert experimental data for reading in GSAS+EXPGUI (2012), which in this work was used to Rietveld refinement method. The average size of the crystallite was determined by two methods: Scherrer and Williamson-Hall, both obtained from the width to half height (FWHM – Full Width at Half Maximum) values of the diffraction peaks. The error check of the crystallographic information file (CIF) obtained by refinement was performed by the Encifer software. The graphic representation of the structure was designed by the software VESTA (Visualisation for Electronic and Structural Analysis) using the crystallographic plugs obtained in the Rietveld refinement for each of the gypsum samples.

3 Results and Discussions

3.1 Scanning electron microscopy

The micrographs obtained by SEM to verify the fracture morphology of the samples of gypsum rocks are shown in Figure 2.

HOLOS
ISSN 1807 - 1600

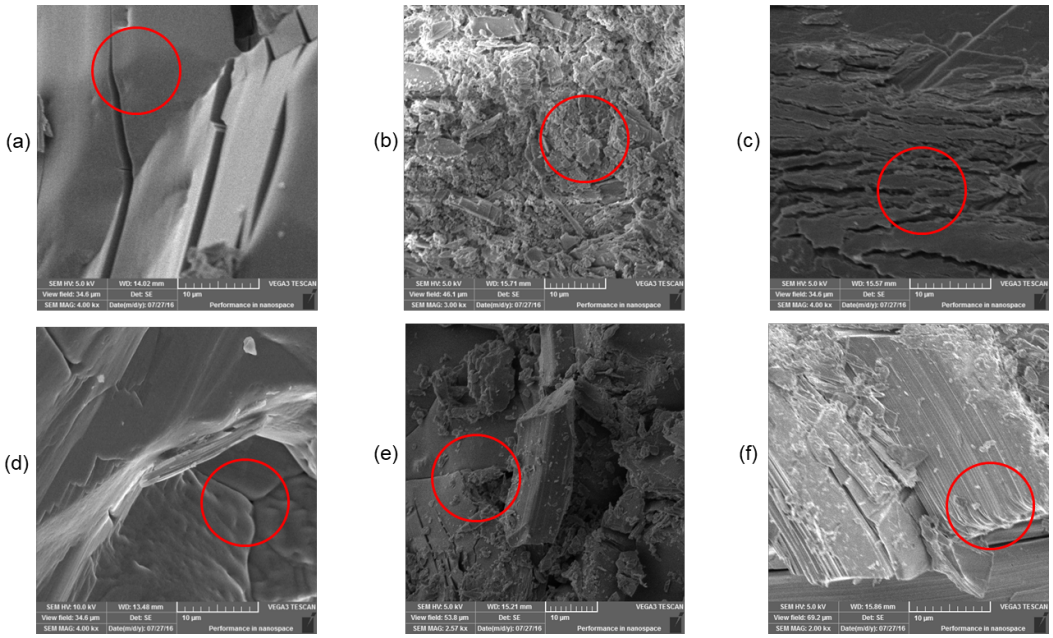

Figure 2: Micrographs of the different varieties of the gypsum mineral: (a) Johnson, (b) alabaster, (c) estrelinha, (d) cocadinha, (e) rapadura and (f) boró.

The Johnson variety, micrograph (a), presents crystals with regular well-structured morphology; micrograph (b) shows the morphology of alabaster, variety with grains of smaller extension; micrograph (c) shows the morphology of the estrelinha variety that presents lenticular crystals; micrograph (d) shows the morphology of the cocadinha variety with horizontal grains; micrograph (e) shows the morphology of the rapadura variety with the presence of surface fragments reminiscent of prismatic grains; and micrograph (f) shows the plate-shaped morphology of the boró variety, the variety that composes the first layer of the gypsum ore.

3.2 X-ray fluorescence

Through XRF, the chemical compositions, in oxides, of the different varieties of gypsum were obtained, as presented in Table 1. It can be observed that the samples, in general, presented a higher mass percentage of oxides that refer to the sulfate and calcium oxide groups, indicating high purity. Besides these oxides, the following were also identified in the gypsum samples: SrO, CuO, P_2O_5, Al_2O_3, MnO, MgO, K_2O, Fe_2O_3, SiO_2 and ZrO_2.

HOLOS
ISSN 1807 - 1600

Table 1: Semi-quantitative analysis of the chemical composition by XRF of gypsum mineralogical varieties.

	GYPSUM ROCK SAMPLE (% WEIGHT)					
Oxides	**Johnson**	**Alabastro**	**Estrelinha**	**Cocadinha**	**Rapadura**	**Boró**
CaO	44.067	45.499	47.061	45.284	44.566	42.530
SO_3	53.217	52.301	48.061	52.060	53.262	52.196
SrO	0.144	0.054	0.284	0.110	0.233	0.090
CuO	-	0.024	0.032	0.028	-	-
P_2O_5	2.121	2.122	1.129	2.066	1.939	1.873
Al_2O_3	-	-	-	-	-	0.731
MnO	-	-	0.099	-	-	-
SiO_2	0.452	-	0.956	0.448	-	2.173
ZrO_2	-	-	-	0.004	-	-
Fe_2O_3	-	-	0.227	-	-	0.235
MgO	-	-	1.750	-	-	-
K_2O	-	-	-	-	-	0.171

According to previous studies (Antunes et al., 2014; Sharpe & Cork, 2006), strontium (Sr) may be associated with the mineral celestine ($SrSO_4$), aluminum (Al), silicon (Si), phosphorus (P), potassium (K) and iron (Fe) may be part of aluminosilicate , zirconium (Zr) may be related to zirconite ($ZrSiO_4$) and magnesium (Mg) may be related to dolomite [$CaMg(CO_3)_2$].

3.3 X-ray diffraction

The experimental data obtained by XRD were compared to the parameters of the Gypsum Reference Sheet (2300259) of the Crystallography Open Database. From the phase analyses performed by the X'Pert HighScore software, the presence of 100% of the gypsum phase was confirmed, corroborating with the high purity observed by the XRF results. The identification of phases in all analyzed samples can be seen in Figure 3.

HOLOS
ISSN 1807 - 1600

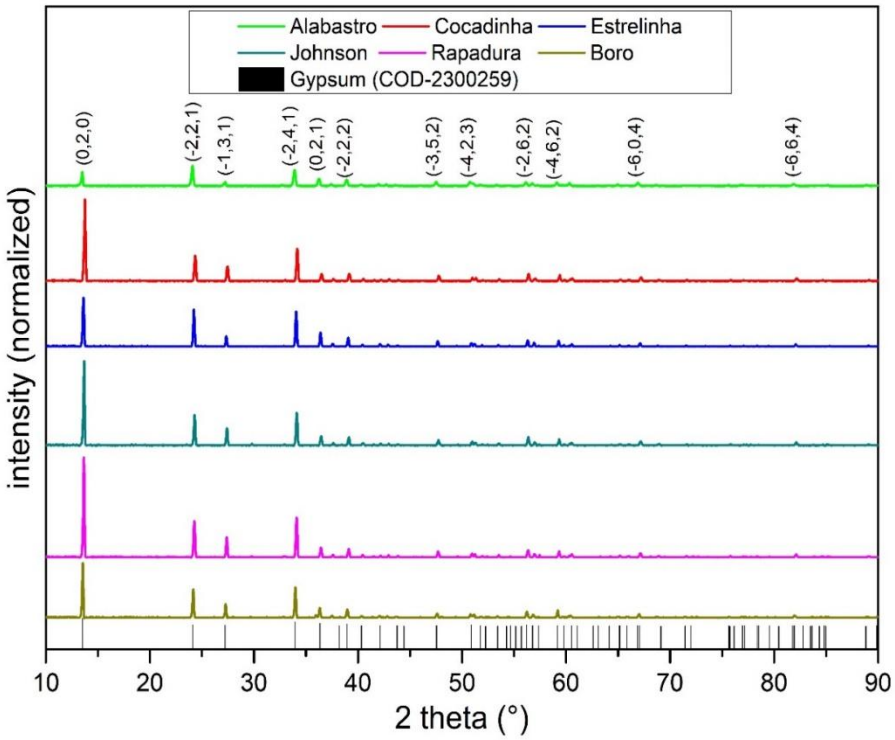

Figure 3: Phase identification and crystallographic planes of gypsum

When the positions of the experimental peaks are compared with the reference standard peaks, it was noted that they have intensity variations, which suggests the presence of preferential orientation in the (020) and (-221) planes, since the analyzed samples are *in natura* minerals. However, the positions at 2θ, show peaks characteristic of gypsum.

Through the Rietveld method refinement it was possible to compare the crystallographic information of the gypsum mineral with the previously chosen crystallographic pattern, and thus verify the fit of the refined model from the graph presented in Figure 4, which shows the result of the refinement of the Johnson type gypsum sample.

HOLOS
ISSN 1807 - 1600

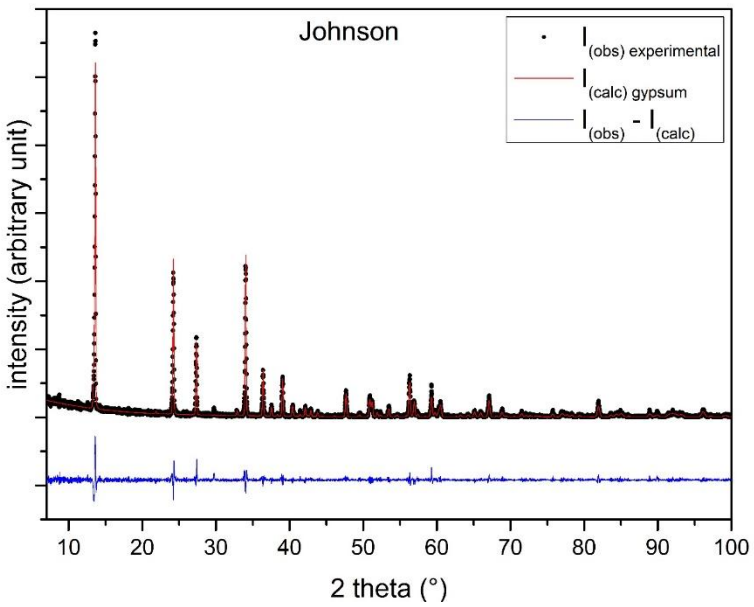

Figure 4: Diffractogram obtained from the refinement by Rietveld method for Johnson gypsum sample. I_{obs}: It represents the intensities of the reference standard and I_{cal} represents the calculated intensities.

In Figure 4 it is possible to see that the relative intensities calculated and observed suffer small deviations, indicating good convergence in the refinement, when the statistical indicators were observed.

Due to the similarity in the results obtained in the Rietveld Refinement the refined diffractograms of all samples can be seen in the supplementary material (Figures S1 to S6).

Table 2 presents the statistical indicators of the refinement expressed in the form of percentage values of the indices: (R_{WP}) weighted profile factor that demonstrates how much refinement is converging; (R_P) or R-standard which is reference value for R_{WP}; (R_F^2) corresponds to the Bragg index and represents the quality of the refined structural model comparing the integrated intensities; and $\chi 2$, which refers to the refinement quality factor. According to the literature, when $\chi 2$ is equal to 1, it means that the calculated spectrum has adjusted perfectly to the experimental spectrum (Young, 1993).

Table 2: Statistical indicators of the refinement

	Gypsum varieties					
	Johnson	**Alabastro**	**Estrelinha**	**Cocadinha**	**Rapadura**	**Boró**
$R_{WP(\%)}$	23.58	26.45	23.38	24.64	24.01	27.44
$R_{P(\%)}$	15.94	18.57	15.86	16.52	16.36	19.23
$R_F^2{}_{(\%)}$	14.21	16.91	13.52	14.78	13.66	18.52
$\chi 2$	0.90	0.87	0.86	0.96	0.98	1.11

HOLOS
ISSN 1807 - 1600

The parameters that measure the quality of the adjustment between the intensities varied as shown in Table 2: the R_{WP} ranged from 23.38% to 27.44% demonstrating the convergence of the refinement in relation to the R_P that ranged from 15.86% to 19.23%, the RP values reflect the expected values for the R_{WP}; the R_F^2 ranged from 13.52% to 18.52% showing how much the structure factor deviated from the standard. The values of $\chi 2$ found in the refinement ranged from 0.86 to 1.11, which makes the refinement result satisfactory when comparing the experimental standard with the reference standard, emphasizing the high crystallinity and purity of the *in natura* gypsum varieties. From this result the anisotropy, crystallite size and gypsum unit cell were obtained.

According to Ungár (2008) the Williamson-Hall chart can be used to qualitatively evaluate the presence of anisotropy. When there is no high dispersion of the points on the chart, it reveals low anisotropy.

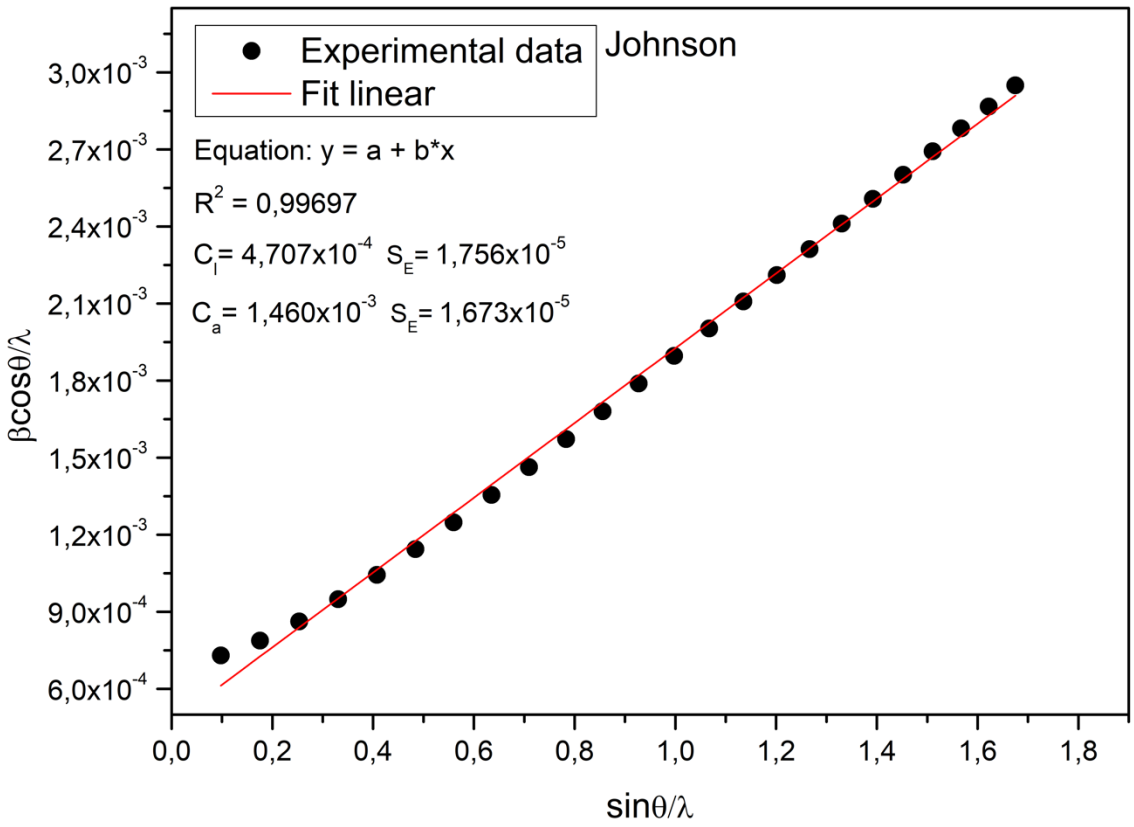

Figure 5: WH plot with the linear fit (R^2), linear coefficient (C_i), angular coefficient (C_a) and standard deviation (S_E) of the Johnson gypsum sample.

From the Williamson-Hall method (WHM) the average crystallite size was calculated, observing the linear coefficient of the curve adjusted to the experimental data. The microdeformation (ε) was determined from the angular coefficient. According to the literature, if the analysis results in a straight line, it indicates a homogeneous sample, if the model does not fit a straight line, it indicates a non-homogeneous sample (Williamson & Hall, 1953).

HOLOS
ISSN 1807 - 1600

From the analysis of the Williamson-Hall graphs of the different types of gypsum, it was possible to observe that the linear fit tends to form a straight line, indicating homogeneous samples for the different varieties of gypsum. Analyzing Figure 5, it can be observed that there was a good linear fit (close to 1.0), which according to Gonçalves et al., (2012), represents homogeneity of crystallite size and microdeformation, indicating that the refractive indices are constant regardless of the direction considered.

The results obtained for the crystallite size of the different gypsum varieties by the Scherrer method were compared with those obtained by the Williamson-Hall method, as shown in Table 3.

Table 3: Crystallite size by the Scherrer method and the Williamson-Hall method

	Crystallite size by method		
Gypsum samples	D (nm) SM	D (nm) WHM	ε
Johnson	55.24	243.90	1.50×10^{-3}
Alabastro	50.38	65.78	4.41×10^{-4}
Estrelinha	61.18	151.74	1.01×10^{-3}
Cocadinha	58.24	179.53	1.18×10^{-3}
Rapadura	58.66	184.80	1.22×10^{-3}
Boró	58.51	221.43	1.35×10^{-3}

According to Table 3, there is a divergence between the values of "D" by Scherrer and Williamson-Hall methods, which was already expected, due to the Scherrer method does not consider the microdeformation in the crystalline network.

According to Gonçalves et al., (2012), when the crystalline structure has a reduced microdeformation, the size determined by the Scherrer equation is close to the real size. It can be observed that for the alabaster variety, which had a smaller microdeformation, both methods showed the closest average crystallite sizes, corroborating the SEM analysis (Figure 2-b), also corroborating the XRD analysis, which showed lower intensity in the planes (0,2,0) and (1,3,1) (Figure 3), which caused a decrease in crystallite size compared to the other samples by WHM.

The different varieties of gypsum correspond to the monoclinic crystal system that has the space group I2/c. The crystallographic parameters are a = 5.67 Å, b = 15.21 Å, c = 6.53 Å, α = 90°, β= 118.484° and γ = 90°. It is observed that the network parameters obtained for the gypsum mineralogical varieties are close to the parameters of the reference standard and corroborate previously performed analyses (Gonçalves et al., 2012; Comodi et al., 2008) that studied synthesized calcium sulfate dihydrate crystals. Comparisons of the lattice parameters for all samples can be seen in Table S1.

Eremin et al., (2016) observed in their experimental analysis the crystallite and microdeformation sizes as respectively, (D) between 120 and 148 nm and (ε) between 1.10 x 10^{-4} and 1.73 x 10^{-3} in their characterization study of calcium sulfate hemihydrates.

The unit cell of gypsum was obtained from the Rietveld method refinement (Figure 6). The unit cell presents 98 atoms forming a total of 12 polyhedra distributed in layers connected by hydrogen bonds. The structure consists of six octahedral sites with the central calcium atom (Ca) and 8 adjacent oxygen atoms (O), and six tetrahedral sites formed by 4 oxygen atoms around the sulfur atom (S). The hydrogens (H) make up the water present in the structure and are attached to the oxygen of the sulfate group belonging to the octahedral site in the unit cell.

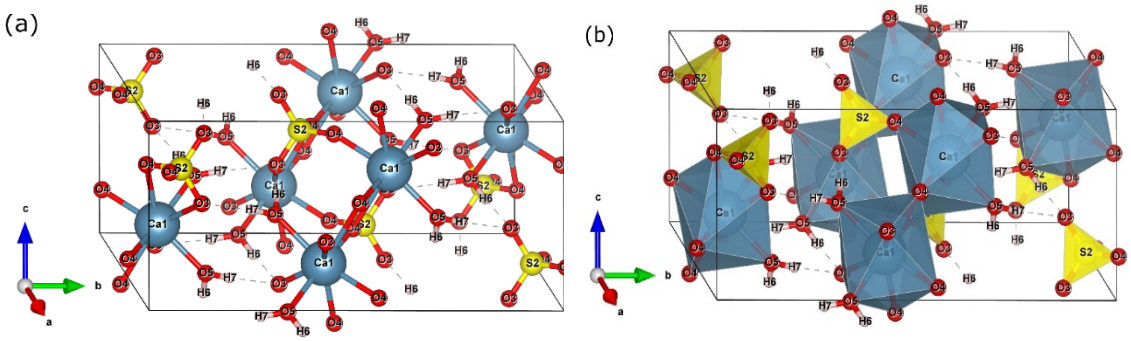

Figure 6: Unit cell of the Johnson gypsum sample (a) ball-and-stick (b) polyhedral view. Atoms are represented by their respective symbols: (S) sulfur, (Ca) calcium, (O) oxygen and (H) hydrogen.

The unit cell obtained from the Rietveld refinement of the majority phase of calcium sulfate dihydrate, as evidenced by XRF and by phase identification by XRD, for all the gypsum varieties were similar. These results reflect that the gypsum varieties analyzed in this study exhibit microstructural similarity. These results corroborate with the results obtained by Fukami et al., (2015) in their synthesis and characterization of calcium sulfate dihydrate, enhancing the results obtained in the macro and microstructural characterization of the gypsum varieties.

4 Conclusion

The characterization of the different varieties of gypsum revealed that, despite the difference in morphology, the chemical compositions of the mineralogical varieties did not present significant variations. Through SEM analysis it was possible to verify that the samples of the gypsum mineral presented different morphologies, indicating a regular placous pattern for the variety known as Johnson and stratified morphology for the alabaster variety.

From the x-ray fluorescence (XRF), it was observed that the samples presented low levels of impurities, confirming the major phase of calcium sulfate dihydrate ($CaSO_4.2H_2O$) by X-ray diffraction (XRD).

Through refinement by the Rietveld method (RM) of the majority phase of gypsum, an acceptable quality adjustment was obtained, with $\chi 2$ close to 1. The crystallite sizes by the different methods calculated (SM and WHM) for the samples analyzed were close to those reported in the literature.

From the refinement it was possible to obtain details about the crystalline structure of the gypsum mineral, such as: the network parameters and the arrangement of the atoms in the unit cell, which confirms, by comparing the techniques used, the high purity of the different types of gypsum and its potential for different fields of application.

5 References

Antunes, V. et al. (2014). Characterization of gypsum and anhydrite ground layers in 15th and 16th centuries Portuguese paintings by Raman Spectroscopy and other techniques. Journal of Raman Spectroscopy, v. 45, n. 11-12, p. 1026-1033.

Bouzit, S. et al. (2019). Characterization of natural gypsum materials and their composites for building applications. Applied Sciences, v. 9, n. 12, p. 2443.

Comodi, P. et al. (2008). High-pressure behavior of gypsum: A single-crystal X-ray study. American Mineralogist, v. 93, n. 10, p. 1530-1537.

Eremin, A. et al. (2016). Determination of Calcium Sulfate Hemihydrate Modification by X-ray Diffraction Analysis. Procedia engineering, v. 165, p. 1343-1347, 2016.

Fukami, T. et al. (2015). Synthesis, Crystal Structure, and Thermal Properties of $CaSO_4.2H_2O$ Single Crystals. International Journal of Chemistry, v. 7, n. 2, p. 12, 2015.

Gonçalves, N. S. et al, M. (2012). Size-strain study of NiO nanoparticles by X-ray powder diffraction line broadening. Materials Letters, p. 36-38, v. 72.

Henry, P. F., Weller, M. T., & Wilson, C. C. (2009). Neutron powder diffraction in materials with incoherent scattering: an illustration of Rietveld refinement quality from non deuterated gypsum. Journal of Applied Crystallography, v. 42, n. 6, p. 1176-1188.

Klein, C., & Dutrow, B. (2012). Manual de ciências dos minerais. 23ed., Bookman. 716p.

Lins, C. A. C. (2018). Informe Geoquímico da Bacia do Araripe: estados de Pernambuco, Piauí e Ceará. CPRM.

Oliveira, F. M. et al. (2012). Características mineralógicas e cristalográficas da gipsita do Araripe. HOLOS, 5, p. 71–82.

Schmid, T., Jungnickel, R., & Dariz, P. (2020). Insights into the $CaSO_4$–H_2O system: A Raman-spectroscopic study. Minerals, v. 10, n. 2, p. 115.

Sharpe R. & Cork G. (2006). Gypsum and anhydrite. In: Kogel JE, Kogel JE et al (eds) Industrial minerals & rocks. Society for Mining, Metallurgy, and Exploration, Inc, Littletown, p 519–540.

Silva, R.; Giulietti, M. (2010). Fosfogesso: geração, destino e desafios. Em: OLIVEIRA, J.; FERNANDEZ, F.; CASTILHOS, S. (eds). Agrominerais para o Brasil. Rio de Janeiro: CETEM; MCT, p 125-144.

Ungár, T. (2008). Dislocation Model of Strain Anisotropy. Powder Diffraction, v. 23, p. 125-132.

Williamson, G. K., & Hall, W. H. (1953). X-ray line broadening from filed aluminium and wolfram. Acta metallurgica, v. 1, n. 1, p. 22-31.

Young, R. A. (1993). The rietveld method. International union of crystallography. Ed. Oxford University Press. v. 5, p. 1-38.

HOW TO CITE THIS ARTICLE
SOUZA, E. D. C., Pessoa Oliveira, R. A., & de Vasconcelos Ferraz, A. . (2023). Characterization of different samples of the gypsum mineral from the Araripe gypsum Pole: from macro to micro with Rietveld refinement. *HOLOS*, *8*(39). https://doi.org/10.15628/holos.2023.14902

ABOUT THE AUTHORS

E.C. SOUZA
Universidade Federal do Vale do São Francisco
E-mail: edjancastro@hotmail.com
ORCID ID: https://orcid.org/0000-0002-1152-442X

R.A.P. OLIVEIRA
Universidade Federal do Vale do São Francisco
E-mail: raquel.oliveira@univasf.edu.br
ORCID ID: https://orcid.org/0000-0002-8455-1226

A.V. FERRAZ
Universidade Federal do Vale do São Francisco
E-mail: andrea.ferraz@univasf.edu.br
ORCID ID: https://orcid.org/0000-0001-8043-1414

Editor responsável: Franciolli Araújo

HOLOS
ISSN 1807 - 1600

Submitted March 14, 2023

Accepted June 16, 2023

Published December 27, 2023

HOLOS
ISSN 1807 - 1600

Associated Content

This material containing additional information about the research will be available free of charge via the Internet.

Rietveld refinement

Through refinement by the Rietveld method it was possible to compare each of the plaster varieties with the standard and to verify the fit of the refined model from the graphs presented in Figures S1 to S6.

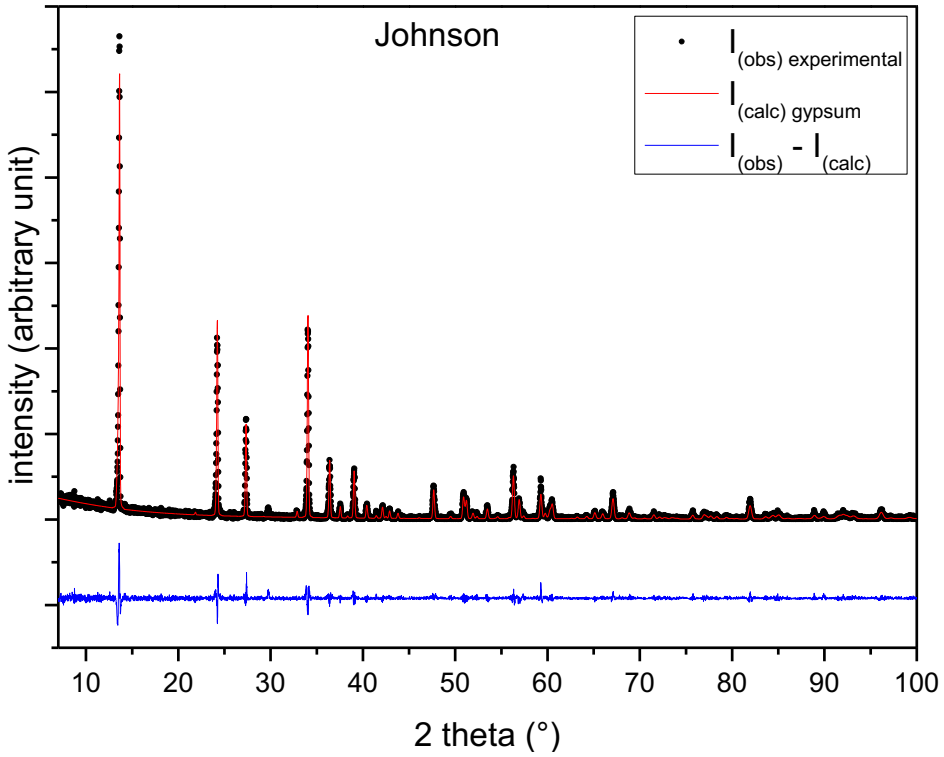

Figure S1 Refined diffractogram for the Johnson sample. I_{obs} represents the intensities of the reference standard and I_{cal} represents the calculated intensities.

HOLOS
ISSN 1807 - 1600

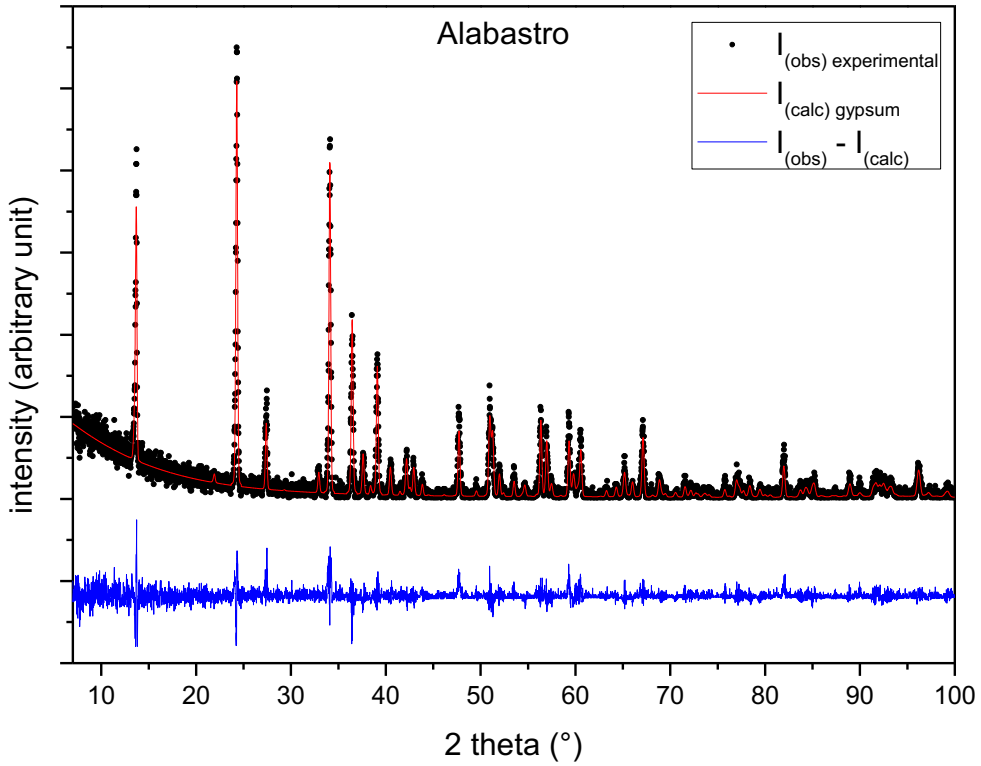

Figure S2 Refined diffractogram for the alabastro sample. I_{obs} represents the intensities of the reference standard and I_{cal} represents the calculated intensities.

HOLOS
ISSN 1807 - 1600

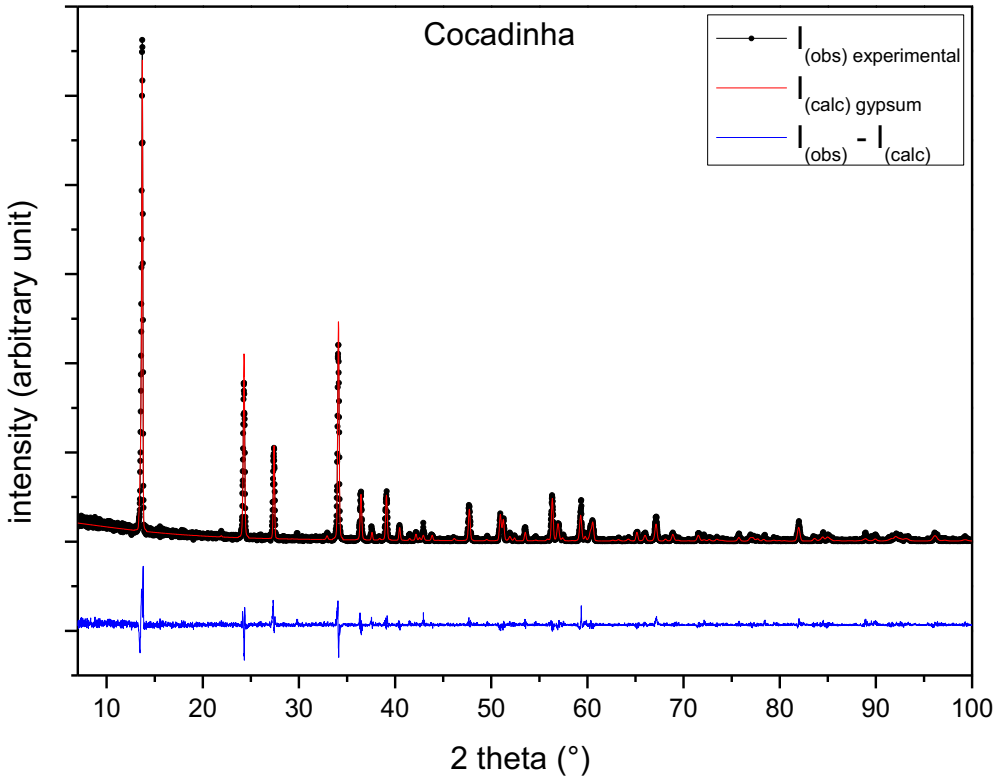

Figure S3 Refined diffractogram for the cocadinha sample. I_{obs} represents the intensities of the reference pattern and I_{cal} represents the calculated intensities.

HOLOS
ISSN 1807 - 1600

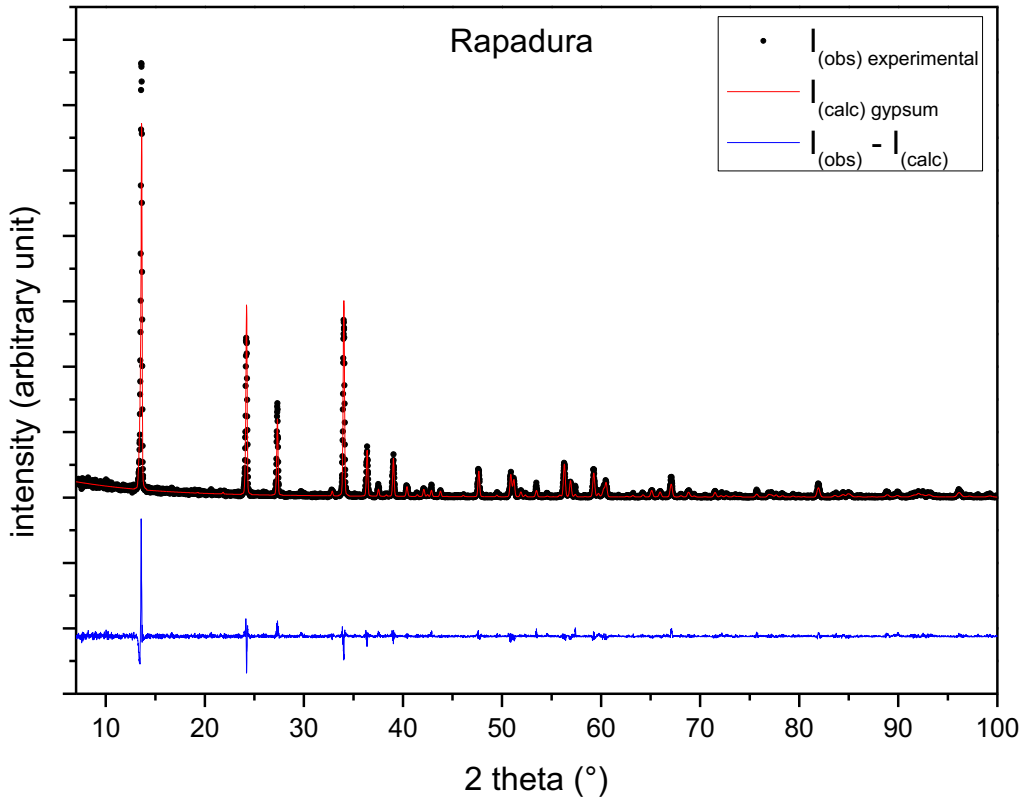

Figure S4 Refined diffractogram for rapadura sample. I_{obs} represents the intensities of the reference pattern and I_{cal} represents the calculated intensities.

HOLOS
ISSN 1807 - 1600

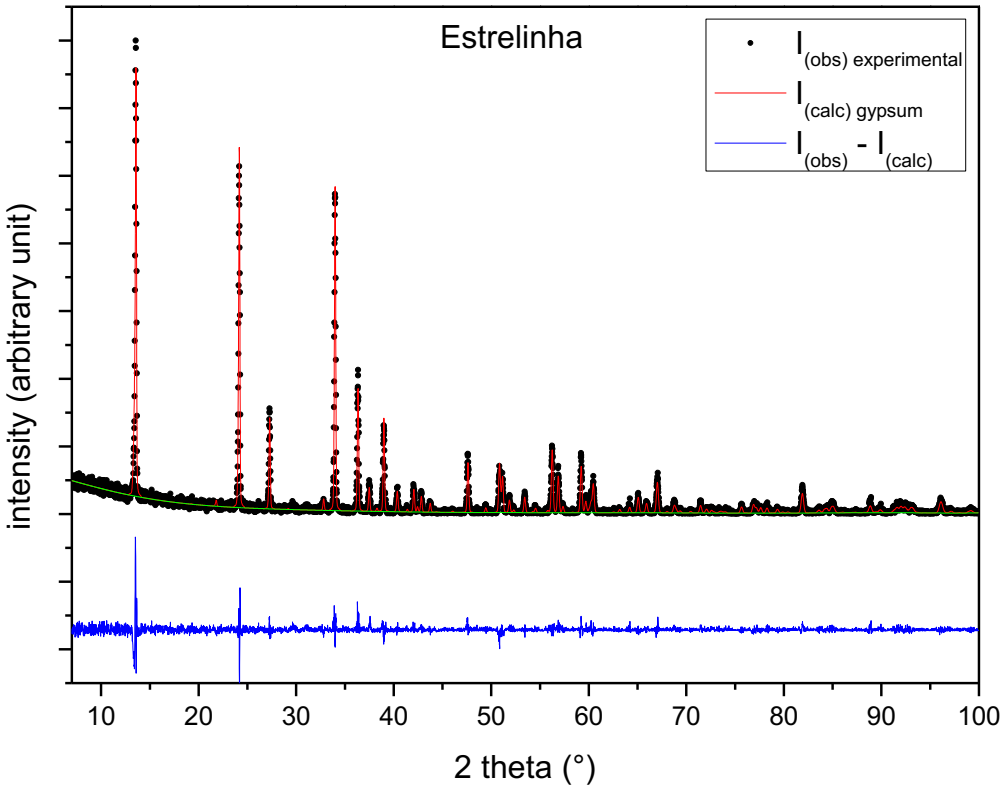

Figure S5 Refined diffractogram for the estrelinnha sample. I_{obs} represents the intensities of the reference pattern and I_{cal} represents the calculated intensities.

HOLOS
ISSN 1807 - 1600

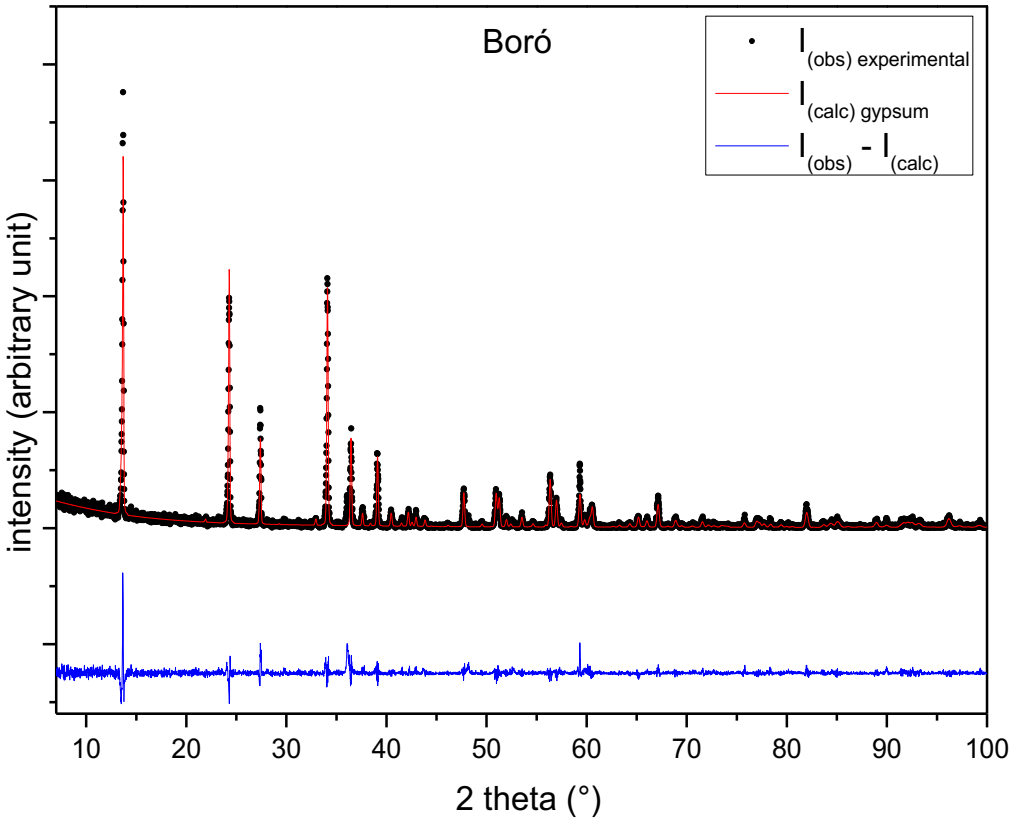

Figure S6 Refined diffractogram for boró sample. I_{obs} represents the intensities of the reference pattern and I_{cal} represents the calculated intensities.

HOLOS
ISSN 1807 - 1600

Crystallographic Data

Table S1 presents the crystallographic data of the gypsum samples, such as: unit cell volume, crystalline system, space group and unit cell dimensions.

Table S1 Crystallographic data obtained from the refinement of the different types of gypsum

Sample	Crystallographic Data			
	Cell Volume ($Å^3$)	Crystalline System	Spatial Group	Unit Cell (Å)
Johnson	495.236	Monoclinic	I 2/c	a = 5.677 b = 15.205 c = 6.526
Alabaster	495.543	Monoclinic	I 2/c	a = 5.677 b = 15.211 c = 6.527
Estrelinha	495.478	Monoclinic	I 2/c	a = 5.678 b = 15.206 c = 6.527
Cocadinha	496.309	Monoclinic	I 2/c	a = 5.682 b = 15.210 c = 6.532
Rapadura	495.322	Monoclinic	I 2/c	a = 5.678 b = 15.205 c = 6.526
Boró	495.132	Monoclinic	I 2/c	a = 5.677 b = 15.204 c = 6.526